Measuring Frequency Dependence and Q-Data of Single Bubble Sonoluminescence in Water

By Philip I. Thomas and Jordan Raisher
Department of Physics Washington University in Saint Louis

Abstract:
Using a commercial kit composed of a cell and variable amplitude horn drive, we demonstrated the basic principles behind Single Bubble Sonoluminescence (SBSL). These principles include the stabilization of sonoluminescent bubbles at pressure anti-nodes, and the correlation between brightness and amplitude. This work verified previous studies. We also demonstrated the temperature dependence of the frequencies required to produce SBSL and established a baseline amplitude range in which SBSL occurs. We also document the appearance of an unexpected two - mode regime around the intended 1-1-3 standing wave condition, both levels of which allowed for sonoluminescence.

I. Introduction

Sonoluminescence (SL) is the phenomenon in which light is produced through the agitation of bubbles using sound. The effect occurs in liquid when stabilized bubbles oscillate through cycles of expansion and compression, theoretically producing regions of high temperature and pressure triggered by cavitation. This cavitation causes chemiluminescence, which is shown to be contingent on the presence of noble gasses.

The effect was first discovered in 1934 by H. Frenzel and H. Schultes during their experiments in underwater sonar at the University of Cologne. Their discovery of acoustically generated light phenomena led to the first studies of Multiple Bubble Sonoluminescence (MBSL) using photographic plates to detect the low-brightness luminescence. Due to the chaotic generation of bubbles in MBSL, accurate and detailed studies of SL could not be carried out until the isolation of a single bubble by then-graduate student Felipe Gaitan in 1989 at the University of Mississippi in a procedure called Single Bubble Sonoluminescence (SBSL). SBSL was accomplished by establishing a standing acoustic wave whose anti-nodes produced strong enough pressure differentials to stabilize the bubble against the buoyant forces.

The most accepted theoretical model which explains SL is Brenner, Hilgenfeldt and Lohse's shockwave model, which is based on the Rayleigh Plesset equation. In this theory, the boundary of the bubble expands and contracts in accordance with the pressure of the sound wave. During the bubble's expansion, small traces of air dissolved in the water are drawn into the bubble as the pressure drops. The bubble is then forced to rapidly contract, causing an adiabatic shockwave to propagate through the interior of the bubble causing very high temperatures, predicted to be as high as 30,000K. This causes high temperature radiation, experimentally shown to be dependent on the presence of noble gasses in the dissolved air. However, due to water's absorption of high-frequency light, a full emission spectrum of the bubble has not been precisely observed. The bubbles have been shown to oscillate between a radius of 50 microns and .5 microns at a rate of over 30GHz. This mechanism of light production remains a point of active research, and debate continues on its assumption of sub-Mach contraction speeds.

In our research we primarily attempted to validate the previous qualitative observations of bubble position and amplitude. In addition, we measured the temperature dependence of the frequencies required for SBSL bubble production.

II. Methods and Procedures

The experiment utilized three main procedures. First, water is prepared via the Water Degassing Procedure. Second, bubbles are produced and measured in accordance with the SBSL Isolation Procedure. Third, we measured the Q Values of the apparatus via the Q Value Collection Procedure.

For the purposes of this experiment, there are two regimes of frequency that were shown to create a standing wave in the chamber. The lower regime is defined as existing between 25.92 and 26.21 kHz, and an upper regime is defined as existing between 28.15 and 29.20 kHz. Our research indicates that these two regimes are different modes of the same 1-1-3 standing wave configuration, as further discussed in the Discussion section.

Water Degassing Procedure

The degassing procedure was a three step process composed of boiling, sealing, and chilling, intended to reduce the amount of air dissolved in the water to ~10% of saturation.

We began by bringing ~900mL of distilled and deionized water in a 1L Erlenmeyer flask on to a rolling boil on a hotplate for twenty minutes. Boiling allowed the gasses dissolved in the water to flow into the bubbles before being passed into the open air.

After twenty minutes, the flask was removed from the heat, sealed with a rubber cork and airtight nozzle, and immersed in an ice bath for one hour. This allowed the water to cool with low gas reabsorption. Keeping the amount of dissolved gas low was intended to control bubble formation and to prevent the bubble from rapidly destabilizing due to absorption during the bubble expansion phase. This ice bath also cooled the water into a temperature range which has been shown in previous studies to support SBSL.

SBSL Isolation Procedure

The cell was filled by placing the apparatus at a sharp angle and pouring the water carefully down the side of the container to prevent agitation which could have increased the level of dissolved gas in the water. The tip of the horn drive was then inserted into the center of the cell with the tip between ~.5 cm below the top of the water level.

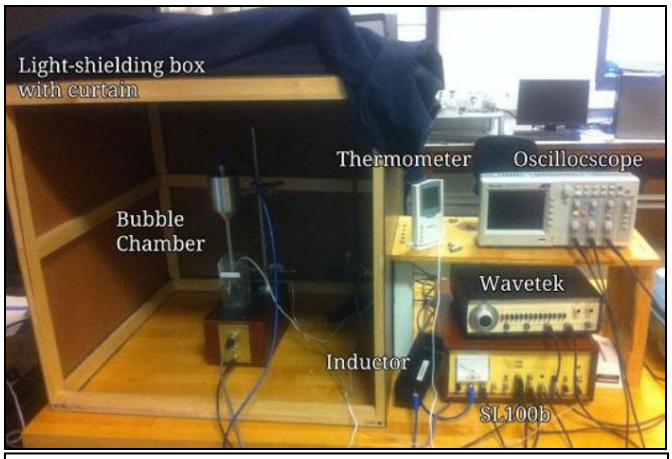

Figure 1: this is the Experimental Apparatus including the Bubble chamber, function generator, oscilloscope and SL100B unit.

After filling the bubble cell (Figure 2) with the degassed water, an acoustic standing wave was established within the chamber. The Wavetek

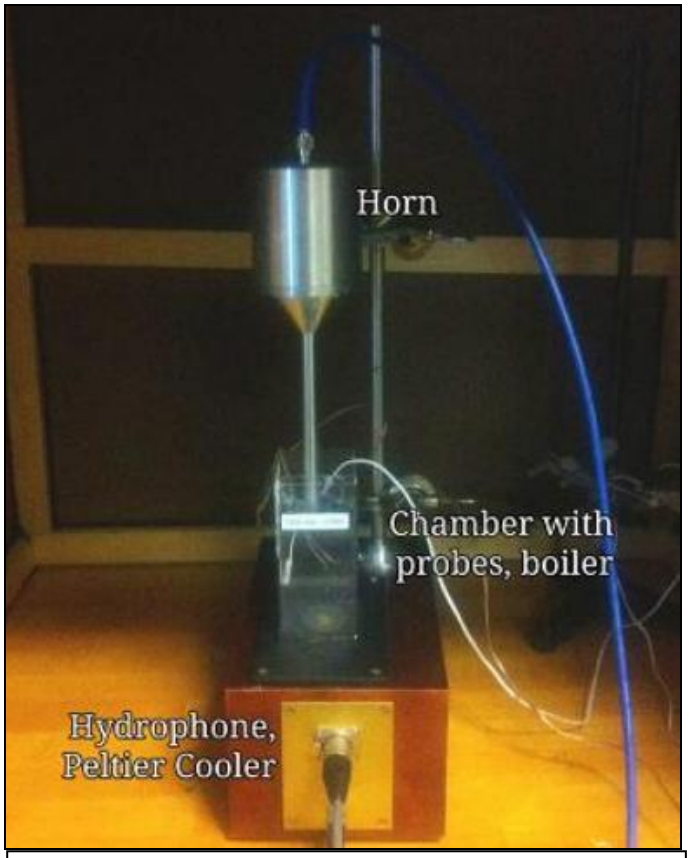

Figure 2: The Bubble chamber including the horn drive, bubble chamber, boiling coil, and probe.

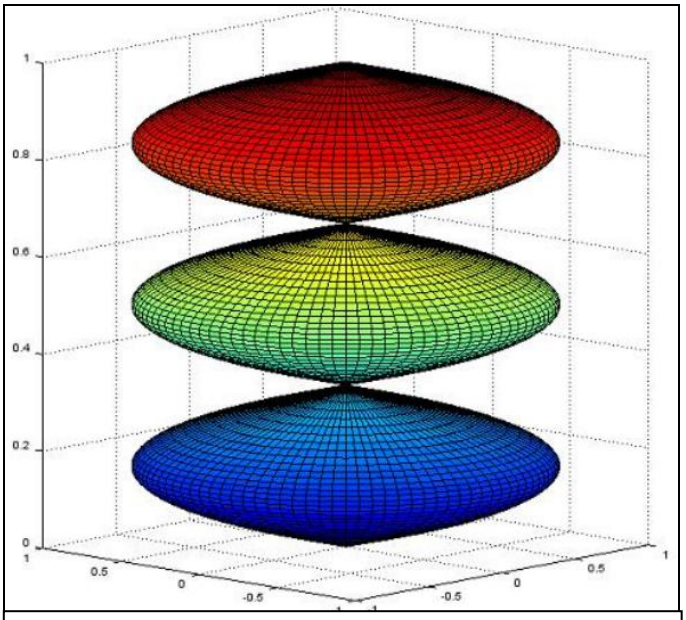

Figure 3: This is a three dimensional visualization of the 1-1-3 harmonic mode along the z axis.

function generator supplied a ~2 Volt, sinusoidal signal at 25 -30kHz in order to establish a 1-1-3 harmonic mode within the 5.4 cm x 5.4 cm x 10 cm cell. This signal was further amplified and specified using the controls on the SL 100B unit before being transmitted to the horn drive. A piezoelectric transducer at the base of the cell allowed for fine-tuning of the signal by producing an output signal which was filtered and directed to an oscilloscope. The 'low frequency' signals could be used to find the maximal pressure amplitude which corresponds to the standing wave condition. The 'high frequency' signal was used in bubble detection (see below).

Upon observation, there appeared to be two standing wave conditions which displayed characteristic 1-1-3 anti-node orientation (Figure 3). The first occurred between the frequencies of 25.92 and 26.21 kHz and will hereby be referred to as the low regime. The second occurred between 28.15 and 29.20 kHz and will hereby be referred to as the high regime. Both regimes displayed two pressure anti-nodes in the lower portion of the cell. However, the higher portion of the cell could not be accurately analyzed to determine the exact wave behavior near the surface and the horn drive itself. A thermometer probe and a boiling filament were inserted into the cell during the trials. The probe was used to record the temperature of the water. Several previous publications indicate that SL becomes more stable at temperatures between 273 K and 293 K. The filament was activated in small pulses of .25-.5 seconds which generated very small bubbles. The pressure amplitude of the horn was varied through the SL 100B unit until SBSL occurred between .5 and 1 second after the use of the boiling filament.

Once produced, a bubble was verified both visually and via the oscilloscope (Figure 4). The oscillation of a stabilized bubble produced a high frequency pressure wave which was displayed on the oscilloscope after passing through the 'high frequency' filter from the piezoelectric transducer. On some occasions, multiple bubbles were stabilized at multiple anti-nodes along the standing wave which could only be reliably identified visually. The amplitude of the horn drive was then decreased to measure the lowest limit at which the bubble was visible, and was then raised to find the amplitude limit at which the bubble became unstable. For each bubble, the water temperature, voltage range, frequency, and number of bubbles produced (1 or 2) was recorded. If no bubble was produced, the frequency and amplitude were changed to reduce auxiliary noise (discussed later) and locate either standing wave condition.

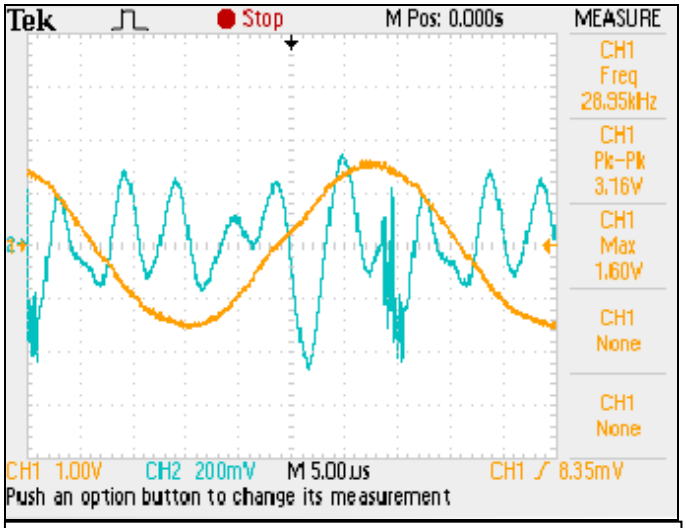

Figure 4: An example of the Oscilloscope reading. The orange curve is the medium frequency piezoelectric signal from the horn drive and the blue wave is the characteristic high frequency bubble signal.

Q Value Collection Procedure

The Q value is a measurement characteristic of the apparatus itself and describes

the precision of the standing wave condition within the cell. This was achieved by measuring the frequency at which the maximal pressure amplitude occurred (ω_0), and then by varying the frequency to find the half maximum amplitude at frequencies both slightly above and slightly below the maximum (ω_1 and ω_2).

The Q value is mathematically expressed as the ratio of the frequency of the maximum amplitude to the frequency width of the half maxima as shown below.

$$Q = \frac{\omega_0}{|\omega_2 - \omega_1|}$$

In order to assess any temperature dependent variation of the Q value, readings were taken as quickly as possible to prevent significant temperature change between frequency measurements. To ensure a Q value which adequately reflected the conditions of our SL conditions, degassed water was used with the thermometer probe and boiling coil in the cell.

III. Results

Q Value

The Q value was measured over 38 trials distributed equally between the high and low regimes using three separate batches of water. The mean Q value over all the trials is 95.23. For the high regime, the average was slightly higher at 97.51 than the low regime at 92.83. The range of values fell primarily between Q values of 41 and 145. While local trends were observed, no reliable temperature or frequency dependence was observed (Figures 5 and 6).

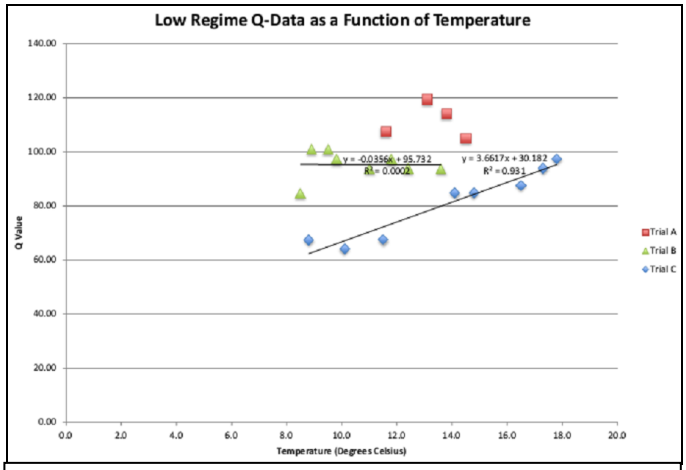

Figure 5: The Q values of the Lower Frequency Regime.

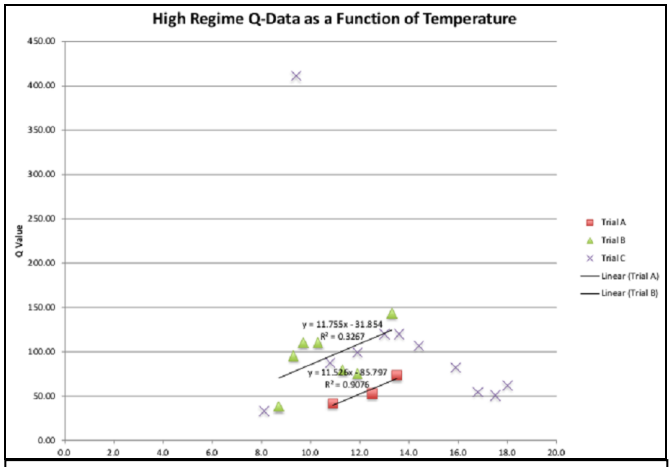

Figure 6: The Q values of the High Frequency Regime.

Amplitude Range

As mentioned in our methods above, the lower boundary of the amplitude range was recorded at amplitudes too low for optical luminescence or where a bubble was present on the oscilloscope, but not visually identified. The upper bound was measured when the bubble became unstable and vanished both visually and from the oscilloscope.

Over 143 bubble observations we calculated the mean voltage range to be 0.48 Volts as measured by the peak to peak voltage of the oscilloscope. This includes both bubbles which

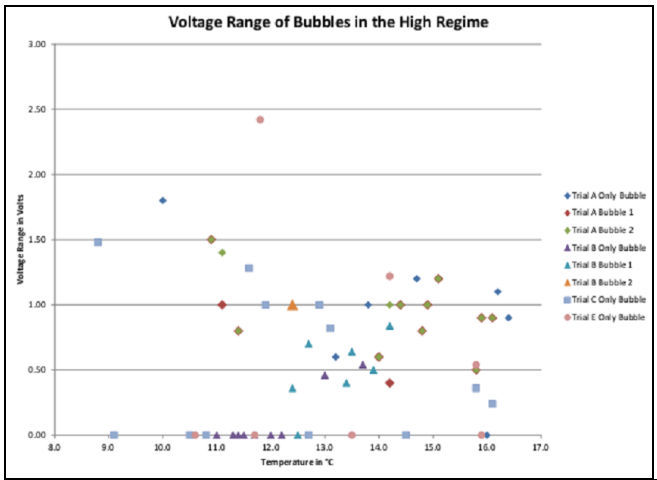

Figure 7: Voltage Ranges of the High Frequency Regime.

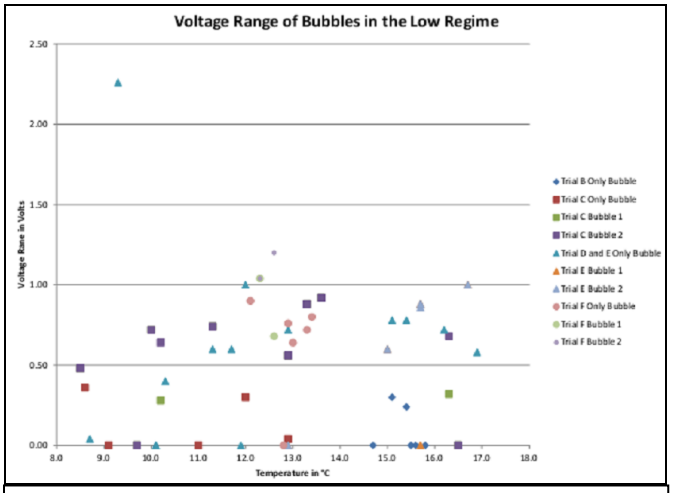

Figure 8: Voltage Ranges of the Low Frequency Regime.

displayed a finite amplitude window and those which were created under unstable conditions and vanished at the same amplitude which they were created. When we include only those bubbles which displayed a finite amplitude window, this average increases to 0.61 Volts as measured by the peak to peak voltage of the oscilloscope over 101 bubbles (Figures 7 and 8).

Temperature Dependence

Our 143 bubble trials were divided into their high and low regime subcategories for temperature dependent analysis. This included a group of 76 bubbles in the high regime and 67 bubbles in the low regime. Frequencies at which bubbles were observed were plotted as a function of temperature. Each regime was further divided into the individual set of trials using the same batch of degassed water (Figures 9).

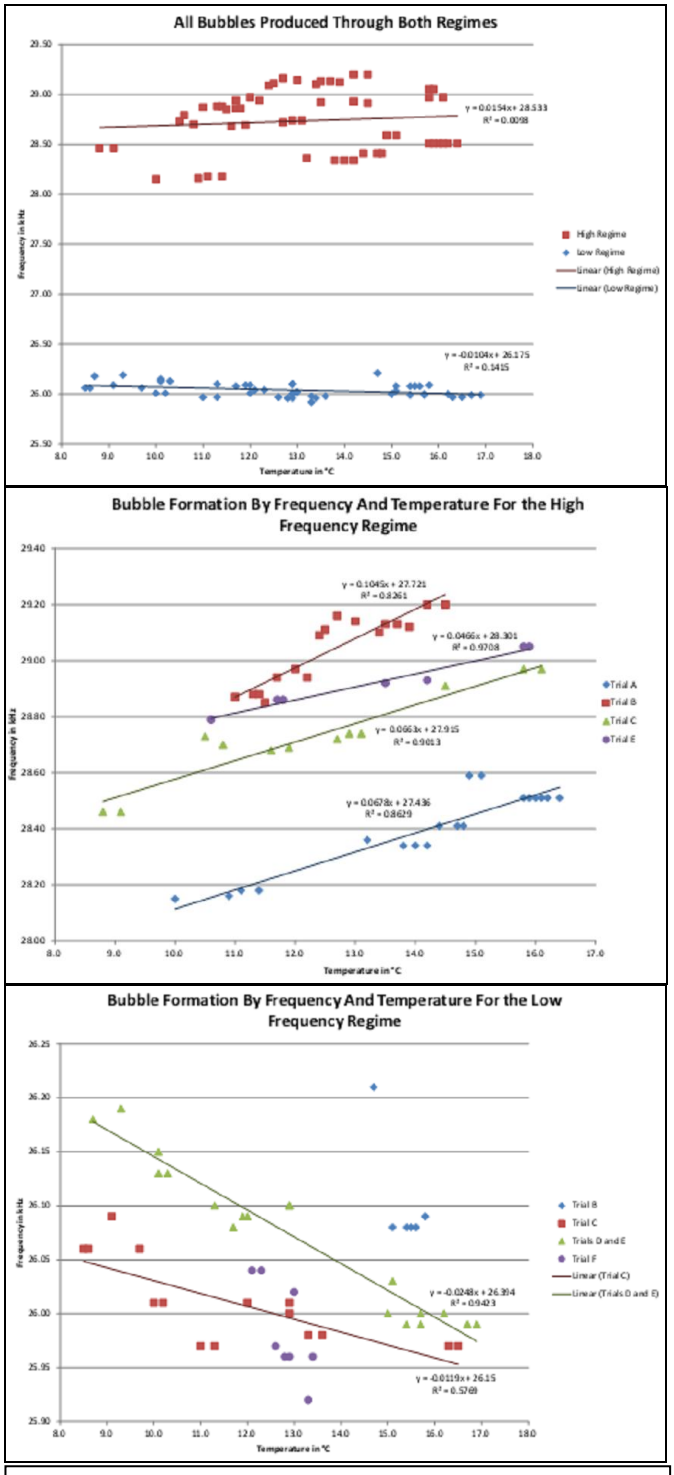

Figure 9: Three graphs demonstrating the correlations in each regime. All bubbles divide into two regimes (top). The high regime bubbles display a positive temperature correlation (middle) and the low regime bubbles display a negative temperature correlation (bottom)

IV. Discussion

Verification of Previous Research

Our main goals of verifying qualitative claims made about SL by previous research groups were accomplished. Through visually examining the luminosity of the bubble in each trial as the pressure amplitude was manipulated, we confirmed that as the amplitude increased, and while still

below the stable limit, the luminosity of the bubble would increase as well. This qualitative assessment can be quantified in the future through the use of a Photomultiplier tube (see below). Simultaneously, in demonstrating that below certain amplitudes, bubbles failed to visually luminesce and above certain amplitudes, the bubbles became unstable, we confirmed the previous claims that SL occurs only in a specific range of pressure amplitudes.

Through observation, we also confirmed that the bubbles were stabilized at the pressure anti-nodes of the system. This was supported by demonstrating the location of the pressure anti-nodes using a hydrophone to qualitatively measure the pressure nodes in the cell.

Data Interpretations

For the majority of tests, we have shown that there is no reproducible correlation between various parameters of this experiment such as between Q value and temperature, Temperature and number of bubbles produced, temperature and amplitude range, number of bubbles produced, and amplitude range, etc. Our clearest correlations, however, were evident in the correlations with the frequency and the temperature. In the high regime, there was a convincing and reproducible positive linear correlation between the temperature and the frequency required to produce SL ($R^2 > .8262$) independently for each trial. In the lower regime, however, we found exactly the opposite trend with a reliable and convincing negative correlation between the temperature and the frequency required for SL ($R^2 = .9423$ and .5769). This indicates that, at least for this apparatus, the fluid dynamics of the system are not fully understood or simply dependent on the temperature (one example being if the frequency were dependent only on the speed of sound in liquid). The specific causes of these divergent correlations are still unknown and were outside the scope of this experiment.

Errors and Further Research

Beginning the experiment, we intended to quantify the luminosity of bubbles as a function of frequency, temperature, and amplitude. However, our attempts to utilize the photomultiplier tube (PMT) were hampered. The first photomultiplier did not provide any signal, and after replacing it, the replacement also yielded no signal. After testing the adapter that converted the PMT output into a coaxial cable output using a digital multimeter, we found that the sheath of the coaxial cable did not correspond to any of the pins from the input of the adapter. While it is possible for a high voltage to not provide a full current loop, the design of the PMT system made it apparent that the system required a full current loop. This led us to believe that the PMT adapter was faulty, and we lacked enough time to replace the item and conduct the luminosity trials.

Quantitative Error

Source	Precision
Thermometer	± 1 ºC
Frequency (Oscilloscope)	± 0.005 kHz
Voltage (Oscilloscope)	± 0.1 V

Using the Theory of Error Propagation, the mean Q value has an error of ± 0.009.

Qualitative Error

During our research we identified several systematic errors within the experimental apparatus which created difficulty and potential further inaccuracies in our observations. The most prevalent source of error was the presence of interference and noise from the horn drive itself. The noise appeared in three ways. First was an audible artifact present in some of the trials. Because the drive frequency exceeded the audible range for a human, the audible noise was most likely a resonant mode of the horn itself. In some but not all cases, physically holding the horn with one's hand was sufficient to dampen the noise further suggesting the horn itself as the source. Second was a high frequency artifact which obscured the bubble signal. Third was a static signal which occasionally would completely obscure the oscilloscope and would disable bubble formation. The horn drive was disassembled, but no loose components were identified.

Via the Water Degassing Procedure, the level of gas saturation in the water is treated in a binary variable - either the water is "degassed" or

it is “expired.” The procedure for water degassing was derived from the Teachspin documentation, and the expected gas level was gleaned from publications. However, the water will slowly reabsorb gas in a continuous manner, and we lacked a way to quantify this change as a continuous variable instead of a binary discrete variable. Hence, error was caused by the inability to control for the reabsorption of air in the water. Future experiments should incorporate a way to control for the level of air in the water.

Due to the design of the circuitry of the SL100b, a low-frequency artifact is present in the piezoelectric transducer that is caused by the resistance of the circuit. This artifact is easily identified when the apparatus is running in the absence of a sonoluminescing bubble. While it caused no known error in our procedure, it is identified for the benefit of future researchers.

The plastic bubble chamber itself was another source of error. One of its walls appears to have been previously cracked and repaired with putty. This means that the shape of the walls may not have been a perfect rectangle, as is assumed in ideal models. Furthermore, the top of the water in the device forms a meniscus, further skewing the ideal rectangular prism shape by introducing a concavity on one of the bounds. Finally, the thermometer and boiler were not incorporated into the models describing the wave propagation in the chamber which may have caused unpredicted aberrations in the wave form. A future chamber could be made which incorporated a boiler and thermometer more efficiently.

V. Conclusions

We have successfully verified the qualitative claims made in previous research projects. We have shown that there is a small range of pressure amplitudes which support SBSL and that, within this range of amplitudes, the luminosity of the bubble is positively correlated with the amplitude of the pressure wave. We also demonstrated that SBSL occurs in the pressure anti-nodes of the standing wave.

We have also demonstrated the strange correlation between temperature and frequency in both standing wave regimes. Ultimately, this is an effect which can provide a topic for future study both in the fluid dynamics of the system itself and the specific properties of sonoluminescence.

VI. References

1. Lohse, Detlef; Fourteen years of single bubble sonoluminescence: A review
2. Crum, Lawrence. "Sonoluminescence." Physics Today. September 1994 22-29.
3. Putterman, Seth. "Sonoluminescence: Sound into Light." Scientific American. February 1995 32-37.
4. Putterman, Seth. "Toward a hydrodynamic theory of sonoluminescence." Phys. Fluids. A.5 (11) (1993): 2911-2927.
5. Brenner, Michael. "Single-Bubble Sonoluminescence." Reviews of Modern Physics. 74. April 2002 (2002): 425-484. Print.
6. SHM notes. Washington University in Saint Louis. Physics 322 Documentation. 2012